Published in final edited form as:
Arterioscler Thromb Vasc Biol. 2014 March ; 34(3): 603–615. doi:10.1161/ATVBAHA.113.303053.

AIP1 mediates VEGFR-3-dependent angiogenic and lymphangiogenic responses

Huanjiao Jenny Zhou[1,2], **Xiaodong Chen**[1,2], **Renjing Liu**[3], **Haifeng Zhang**[1], **Yingdi Wang**[1], **Yu Jin**[1], **Xiaoling Liang**[2], **Lin Lu**[2], **Zhe Xu**[4,5], and **Wang Min**[1,5]

[1]Interdepartmental Program in Vascular Biology and Therapeutics Yale University School of Medicine, 10 Amistad St., New Haven, CT 06520

[2]State Key Laboratory of Ophthalmology, Zhongshan Ophthalmic Center, Sun Yat-sen University, Guangzhou, China

[3]Diseases of the Aorta Lab, Center for the Endothelium, Vascular Biology Program, Centenary Institute and University of Sydney, Sydney, Australia

[4]Department of Ophthalmology, Guangzhou General Hospital of Guangzhou Military Command, Guangzhou. 510010. China

Abstract

Objective—To investigate the novel function of AIP1 in VEGFR-3 signaling, and VEGFR-3-dependent angiogenesis and lymphangiogenesis.

Approach/Results—AIP1, a signaling scaffold protein, is highly expressed in the vascular endothelium. We have previously reported that AIP1 functions as an endogenous inhibitor in pathological angiogenesis by blocking VEGFR-2 activity. Surprisingly, here we observe that mice with a global deletion of AIP1 (AIP1-KO) exhibit reduced retinal angiogenesis with less sprouting and fewer branches. Vascular endothelial cell (but not neuronal)-specific deletion of AIP1 causes similar defects in retinal angiogenesis. The reduced retinal angiogenesis correlates with reduced expression in VEGFR-3 despite increased VEGFR-2 levels in AIP1-KO retinas. Consistent with the reduced expression of VEGFR-3, AIP1-KO mice show delayed developmental lymphangiogenesis in neonatal skin and mesentery, and mount weaker VEGF-C-induced cornea lymphangiogenesis. In vitro, human lymphatic EC with AIP1 siRNA knockdown, retinal EC and lymphatic EC isolated from AIP1-KO all show attenuated VEGF-C-induced VEGFR-3 signaling. Mechanistically, we demonstrate that AIP1 via *vegfr-3*-specific *miR-1236* increases VEGFR-3 protein expression, and by directly binding to VEGFR-3 enhances VEGFR-3 endocytosis and stability.

Conclusion—Our in vivo and in vitro results provide the first insight into the mechanism by which AIP1 mediates VEGFR-3-dependent angiogenic and lymphangiogenic signaling.

Keywords

AIP1; VEGF; VEGFR-2; VEGFR-3; lymphangiogenesis; vascular biology

[5]Corresponding author: Dr. Wang Min, Interdepartmental Program in Vascular Biology and Therapeutics, Department of Pathology, Yale University School of Medicine, 10 Amistad St., New Haven, CT 06520. Tel: 203-785-6047; Fax: 203-737-2293; wang.min@yale.edu and Dr. Zhe Xu at oculistxuzhe@163.com.

Disclosure: None.

Introduction

The vasculature contains blood vessels and lymphatic vessels, two developmentally related but functionally distinct systems. In ontogeny, the prevalent theory is that lymphatic vessels originate from a subset of venous endothelial cells in the anterior cardinal vein that express Sox-18, a member of the Sox family of transcriptional factors critical for cardiovascular development. Sox-18 can turn on expression of homeobox transcription factor Prox-1 around embryonic (E) 9.5 of mouse development to initiate the lymphatic specification program [1, 2]. In addition, Coup-TFII, an orphan nuclear receptor, assists in turning on and maintaining the expression of Prox-1 [3]. After commitment to the lymphatic cell lineage, the Prox-1 positive cells sprout to form the primary lymph sacs. Studies suggest that vascular endothelial growth factor receptor-3 (VEGFR-3) is critical for sprouting and migration in response to its ligand, vascular endothelial growth factor-C (VEGF-C) [4]. Peripheral lymphatic vessels form by centrifugal sprouting from the primary lymph sacs to form a network, followed by maturation of large collecting lymphatic vessels. Lymphatic vessels express distinct cellular markers such as Prox-1, podoplanin [5], and lymphatic vessel endothelial hyaluronan receptor-1 (LYVE-1) [6], However, both blood and lymphatic endothelium express surface receptors VEGFR-2 and VEGFR-3 [7]. VEGFR-2 plays an essential role during vascular development. It is also required for lymphatic endothelium organization into functional capillaries [8–10]. On the other hand, VEGFR-3 is expressed in the blood endothelium during development, and is restricted to the lymphatics in the adult with the exception of few blood capillaries in some organs [11–13]. Therefore, VEGFR-3 is critical for both developmental angiogenesis and lymphangiogenesis. It has been reported that VEGFR-3 null mice die as early as E10.5 prior to the formation of the lymphatics system due to a failure in remodeling of the primary vascular plexus [14]; VEGFR-3 is expressed in angiogenic retinal vessels, and blockade of VEGFR-3 signaling blunts retinal vessel growth [7, 15]. When deficient in the VEGFR-3 ligand VEGF-C, mouse embryos are deprived of primitive lymph sacs and all other lymphatic vessels and die after E15.5 [4]. In humans, congenital hereditary lymphedema known as Milroy disease has been linked with a mutation in the tyrosine kinase domain of the VEGFR-3 gene[16, 17]. Similarly, the *Chy* mouse mutant, a model for congenital lymphedema that contains a heterozygous mutation to deactivate VEGFR-3, has abnormal cutaneous lymphatic vessels and symptoms of lymphedema [18]. Despite the importance of VEGFR-3 in the developing angiogenesis and lymphangiogenesis, regulation of VEGFR-3 expression and activity during development remains poorly understood.

The signaling pathways induced by the VEGF family of ligands and their receptors have been investigated [19, 20]. Most of our current understanding of VEGFRs signaling have been from VEGFR-2 studies. Specifically, VEGF-A rapidly induces VEGFR-2 dimerization and autophosphorylation (pY1054/59 and pY1175) followed by the activation of phosphatidylinositol 3-kinase (PI3K)-Akt, phospholipase C-gamma (PLC-γ) and MAP kinase, leading to biological responses such as survival, proliferation, and migration. Similarly, in response to its ligands (VEGF-C), VEGFR-3 is phosphorylated at its C-terminal tyrosine residues. While VEGFR-2 activity is positively or negatively regulated at multiple steps by interacting proteins, intracellular trafficking, phosphatases and microRNAs [21–25], intracellular signaling mediators for VEGFR-3 are less characterized.

AIP1, a novel signaling scaffolding protein, is highly expressed in the vascular endothelium during mouse development and in adult. AIP1 is also abundantly expressed in some neuronal cells [26, 27]. Although AIP1 was initially identified as an ASK1-interacting protein, it contains multiple structural domains including the pleckstrin homology (PH) domain, the protein kinase C conserved region 2 (C2) and RasGAP at its N-terminus while a proline-rich sequence (PR), a coiled-coil and leucine-zipper motif (CC/LZ) as well as phospho-serine

sites for the 14-3-3 and Akt binding can be found at the C-terminus [28]. We have shown that mice with a global AIP1 deletion (AIP1-KO) exhibit dramatically enhanced atherosclerosis and graft arteriosclerosis in animal models [27, 29, 30]. These phenotypes in adult AIP1-KO mice largely attribute to enhanced inflammatory responses (endothelial activation, macrophage infiltration and cytokine production). In agreement with this, in vitro data demonstrate that AIP1 can act as an inhibitor in several pro-inflammatory pathways including the TNF [31, 32], Toll-like receptor-4 [33] and IFN-γ signaling pathways [29]. AIP1-KO adult mice also exhibit enhanced ischemia and inflammation-induced angiogenesis by associating with VEGFR-2 and inhibiting the VEGFR-2-dependent signaling [27]. However, the role of AIP1 in vascular development has not been carefully examined. In the present study, we were surprised to observe that mice with either a global or an endothelial-specific deletion of AIP1 displayed delayed vascular development of both retinal angiogenesis and lymphangiogenesis. These defects are specifically the result of reduced VEGFR-3 expression (but not VEGFR-2) in the vascular endothelium. Our data demonstrate that AIP1 modulates VEGFR-3 protein expression, endocytosis and stability, uncovering that AIP1 is a novel regulator in VEGFR-3 signaling.

MATERIALS AND METHODS

Materials and Methods are available in the online-only Data Supplement.

Results

AIP1-KO mice show reduced retinal angiogenic sprouting

We have previously established the AIP1-flox (*AIP1*$^{lox/lox}$) mice using homologous recombination [27]. Global AIP1 knockout (AIP1-KO) mice were subsequently generated by mating the AIP1$^{lox/lox}$ mice with the β-actin-Cre deleter mice. These mice were viable with normal gross growth. However, further examinations indicated that the AIP1-KO mice show delayed vascular development during embryonic and neonatal stages. Specifically, AIP1-KO embryos exhibited delayed maturation of vasculature throughout the body including the head and skin (Supplemental Fig. I for E13.5). Retinal angiogenesis provides a good model for the analyses of the kinetics of vascular development [34]. The superficial retinal vascularized areas in the ganglion cell layer (GCL) of WT and AIP1-KO mice at various postnatal days were measured by isolectin staining and quantified as a percentage of the total retinal surface. As illustrated in a schematic diagram in Supplemental Fig. IIa and isolectin staining in Supplemental Fig. IIb, the vasculature in WT mouse grew from the optical center towards the periphery of the retina during development. The vasculature front reached one third of the retina on postnatal days 3 (P3), leaving the rest of the retina completely avascular. The vasculature front reached two thirds of the retina on P7, and nearly reached the retina edge by P9. AIP1-KO mice displayed a significant delay in the radial extension of the vascular plexus from the optic nerve to the periphery from P4 (Fig. 1A with quantification in 1B) to P7 (Supplemental Fig. IIb with quantification in Fig. IIc). Endothelial tip cells localized at the retinal front during development are characterized by specialized apical filopodia and are vital for the development of new capillaries [35]. AIP1 deletion significantly reduced the number of tip cells as visualized by high power images of the vascularization regions (Fig. 1C with quantification in 1D). Although coverage of the retina by the primary vascular layer in AIP1-KO mice was complete and similar to WT mice at P9 (Fig. 1E), the development of the deeper intraretinal vessels which originates from the GCL into the inner plexiform layer (IPL) and outer plexiform layer (OPL) were also delayed in the AIP1-KO mice compared to WT pups (Fig. 1F with quantification in Fig. 1G). These data suggest that AIP1 deletion delays retinal vascular development. We then examined EC proliferation which is critical for retinal angiogenesis [34]. Proliferative EC were first detected

by whole mount staining with isolectin and anti-phosphor-histone H3 (pH3), a marker for mitosis. The $pH3^+$ cells were significantly reduced in the AIP1-KO retinas (Fig. 1H with quantification in 1I). EC proliferation was also examined by BrdU incorporation which visualizes DNA replication. WT and AIP1-KO pups were injected with BrdU for 2 h and retinas were harvested for whole mount staining with anti-BrdU. Similarly, AIP1-KO retinas had drastically reduced $BrdU^+$ cells compared to WT retinas (Fig. 1J with quantification in 1K). These data indicate that AIP1 deletion delays retinal angiogenesis by reducing EC proliferation.

AIP1 in vascular endothelial cells plays an important role in retinal angiogenesis

Previously we have shown that AIP1 is highly abundant in vascular endothelial cells (EC) [26, 27]. We generated the EC-specific AIP1-knockout mice (AIP1-ecKO) mice by mating the $AIP1^{lox/lox}$ mice with Tie2-Cre deleter mice. EC-specific deletion of AIP1 in the AIP1-ecKO retina were detected by whole mount and cross-sectional immunostaining. In WT mice, AIP1 protein was primarily detected in the vascular endothelium of retina where it was co-localized with isolectin staining; WT shows >99.5% co-staining of AIP1 and isolectin based on the cross-sectional staining. AIP1 staining was absent in AIP1-ecKO retinas (Fig. 2A–B). AIP1-ecKO mice reproduced the delay in retinal vessel growth (Fig. 2C with quantification in Fig. 2D) with fewer tip cells (Fig. 2E with quantification in Fig. 2F) as observed in the AIP1-KO mice. AIP1 deletion appeared to have no significant effect on the pericyte coverage in retinas (Fig. 2G). GFAP staining for astrocytes indicated no alterations in astrocyte morphology and astrocyte-EC interactions in AIP1-ecKO retinas compared to WT retinas (Supplemental Fig. III).

Retinal angiogenesis can also be regulated by neuronal cells [34]. AIP1 has been reported to be expressed in subsets of neuronal cells such Purkinje cells in the mouse brain [27]. To determine if AIP1 is expressed in retinal neuronal cells and explore the potential role of neuronal AIP1 in retinal angiogenesis, we generated the AIP1-nKO by mating the $AIP1^{lox/lox}$ mice with Nestin-Cre deleter mice [36] to specifically inactivated *AIP1* in neuronal cells. The specificity of Nestin-Cre for neuronal cells was previously confirmed by breeding Nestin-Cre deleter mice with mice expressing a genetic Cre reporter (ROSA26YFP) in which Cre-mediated recombination leads to the expression of yellow fluorescence protein (YFP) specifically in the retinal astrocytes but not in the retinal endothelium in the whole mount staining [37]. Consistent with the results in Fig. 2, AIP1 was primarily detected in retinal endothelium but absent in neuronal cells in WT mice, and AIP1 expression was unchanged in the AIP1-nKO retinas as demonstrated by the staining (Fig. 3A–B). Importantly, retinal angiogenesis was normal in the AIP1-nKO mice (Fig. 3C with quantifications in 3D). Taken together, these results suggest that AIP1 is primarily expressed in retinal endothelial cells where it plays a critical role in the retinal angiogenesis.

VEGFR-3 is specifically reduced in AIP1-KO retinas

The delay in retinal angiogenesis with fewer tip cells have been associated with reduced VEGFR-2/VEGFR-3 activity or enhanced Notch signaling [7, 15, 38–40]. We first examined the expression of the Notch receptors and ligands as well as the Notch downstream targets Hes and Hey1. We did not detected significant changes in the expression of Notch receptors, Notch ligands or the Notch targets (Fig. 4A). Although the mRNA levels of VEGFR-2 and VEGFR-3 were not altered, VEGFR-2 and VEGFR-3 proteins were evidently affected by the AIP1 deletion. While VEGFR-2 expression was increased from P5 to P7 in the AIP1-KO retinas, VEGFR-3 was significantly reduced by AIP1 deletion at these stages. Expressions of both VEGFR-2 and VEGFR-3 were at similar levels between WT and AIP1-KO retinas after P8 (Fig. 4B with quantifications in 4C). These data suggest that the level of VEGFR-3, but not that of the Notch receptors/ligands or VEGFR-2, correlates with the angiogenic

phenotype in the AIP1-KO retinas. To determine effects of AIP1 on VEGFR-2 and VEGFR-3 are EC intrinsic, we examined the VEGFR-3 expression and VEGF-C signaling in isolated retinal EC. As observed in retinal whole lysates, expression of VEGFR-3 was reduced in the AIP1-KO retinal EC. VEGF-C-induced phosphorylations of VEGFR-3 and downstream Akt were also reduced in AIP1-KO retinal EC (Fig. 4D).

AIP1 deletion delays VEGFR-3-dependent lymphangiogenesis

Besides playing an important role in retinal angiogenesis, lymphatic sprouting and valve formation are also highly dependent on VEGFR-3. We therefore determined the effects of AIP1 deletion on lymphangiogenesis in neonatal skin and mesentery. Immunostaining of the foreskin and mesentery tissues with vascular markers demonstrated that both blood capillary network and lymphatic vessels had less density and fewer branches in the AIP1-KO mice (Fig. 5A with quantifications in Fig. 5B–C). Consistent with the published data that VEGFR-3 is highly expressed in sprouting retinal vessels, VEGFR-3 was strongly expressed in newly sprouting lymphatics in WT mice, but was significantly reduced in AIP1-KO mice (Fig. 5D). We also examined development of collecting lymphatic vessel and lymphatic valve formation in the AIP1-KO mice. The development of mesenteric collecting lymphatic vessels starts from E15.5, when a mesh-like network of lymphatic vessels is formed by lymphatic EC surrounding the mesenteric arteries and veins. By E17.5, lymphatic vessel trunks are formed and exhibit the presence of luminal valves. By E18.5, the luminal valves further mature to V-shaped valve leaflets which are formed by Prox-1 positive lymphatic endothelial cells [41]. We observed typical mature leaflets of mesentery lymphatics in WT mice at P0 characterized by increased VEGFR-3 expression. AIP1-KO mice at P0 displayed reduced VEGFR-3 expression, dilated lymphatic vessels with incomplete or diffused valve formation (Fig. 5E). We confirmed that AIP1-KO P0 skin/mesentery tissues had reduced VEGFR-3 protein expression by Western blots (Fig. 5F). To directly determine whether AIP1-KO mice are specifically defective in VEGFR-3 signaling, we employed cornea lymphangiogenesis assays induced by a mutant form of VEGF-C (C156Ser; CS) that binds to and activates VEGFR-3 but not VEGFR-2. The mammalian cornea is one of only a few avascular tissues in the body. Both angiogenesis and lympangiogenesis could be induced by implantation of VEGF-containing Hydron pellet into the center of cornea [42–44] (Supplemental Fig. IV-A). VEGF-CS induced sprouting of both blood and lymphatic vessels from the preexisting corneal limbus as visualized by CD31 and LYVE-1 staining, and AIP1-KO corneas exhibited reduced VEGF-CS responses compared to WT on day 14 post-implantation when lymphangiogenesis peaked [42–44] (Supplemental Fig. IV-B with quantifications in C,D). These results support a role for AIP1 in VEGF-C-induced cornea lymphangiogenesis.

AIP1 mediates VEGF-C/VEGFR-3 signaling and function in human lymphatic endothelial cells

To determine the mechanism by which AIP1 regulates VEGFR-3 signaling, we determined the effect of AIP1 knockdown on VEGFR-3-mediated lymphangiogenesis in cultured human lymphatic endothelial cells (HLEC). We have previously characterized HLEC for expression of the lymphatic EC markers (Prox-1, LYVE-1 and podoplanin) and VEGFR-3 signaling [42–44]. All experiments were performed in early passages (passages 3–6) and cells remained Prox-1 positive and VEGF-C responsive. VEGFR-3 has been shown to be important for migratory signals in HLEC [45]. Therefore, we determined if AIP1 knockdown affects HLEC migration. A control or AIP1 siRNA was transfected into HLEC, and cell migration was assessed by a scratch wound assay in response to VEGF-CS. AIP1 siRNA significantly reduced scratch closure by HLEC in response to VEGF-CS compared to the control siRNA (Fig. 6A with quantification in 6B). To determine if AIP1 directly regulates EC proliferation as we observed in retinas, we performed in vitro BrdU incorporation assays

in AIP1 knockdown HLEC. Under normal culture media with growth factors, AIP1 siRNA-transfected HLEC showed significantly reduced $BrdU^+$ cells compared to the control siRNA group (Fig. 6C with quantification in 6D), suggesting that AIP1 deletion reduced EC proliferation. We then examined the role of AIP1 expression in VEGFR-3 expression and signaling which is critical for lymphatic EC proliferation and migration. Consistent with results from AIP1-KO tissues, knockdown of AIP1 drastically reduced the protein level of VEGFR-3 (by 50–70% for the 125 kDa mature form) with slightly increased VEGFR-2 expression. AIP1 siRNA had no effects on VEGFR-3 mRNA levels in HLEC (data not shown), suggesting that AIP1 regulates VEGFR-3 at a protein level. AIP1 knockdown also blunted VEGF-CS-induced phosphorylation of VEGFR-3 and the major downstream effector Akt (Fig. 6E with quantifications below each blot). We observed similar effects of AIP1 siRNA on VEGFR-3 signaling induced by wild-type VEGF-C (Fig. 6F). Of note, VEGF-C, but not VEGF-CS, weakly activated phosphorylation of VEGFR-2 which was slightly augmented by AIP1 knockdown. Reduced VEGFR-3 expression and signaling were also observed in the mouse lymphatic EC isolated from AIP1-KO skin compared to WT (Fig. 6G). Importantly, the defect in VEGFR-3 signaling induced by AIP1 deletion was rescued by re-expression of AIP1 (Supplemental Fig. V for overexpression of murine AIP1 cDNA in hAIP1 siRNA-transfected HLEC).

AIP1 regulates both VEGFR-3 protein expression and VEGFR-3 activation

AIP1 deletion appears to have a profound effect on the VEGFR-3 protein but not its mRNA level. We have recently shown that *miR-1236* binds to the 3′ untranslated region (UTR) of the *Vegfr3* mRNA and inhibits its translation [42]. We measured *miR-1236* levels in HLEC with control and AIP1 siRNA. AIP1 knockdown in HLEC significantly augmented *miR-1236* expression (Fig. 7A), indicating AIP1 may control the VEGFR-3 protein level via repressing *miR-1236*.

While AIP1 deletion reduced the protein level of VEGFR-3 by 50–70%, the effects of AIP1 deletion on phosphorylation of VEGFR-3 and its downstream Akt were greater (Fig. 5&6), suggesting that AIP1 may also directly regulate VEGFR-3 signaling. To this end, HLEC were untreated or treated with VEGF-C. The associations of AIP1 with VEGFR-3 were determined by a co-immunoprecipitation assay. Consistent with previous findings, AIP1 associated with VEGFR-2 only after VEGF treatment. In contrast, AIP1 and VEGFR-3 complex was detected in resting HLEC (Fig. 7B), indicating that AIP1 constitutively associates with VEGFR-3. To directly determine the effects of AIP1 binding on VEGFR-3 expression and activity, FLAG-tagged expression constructs encoding different AIP1 structural domains (the full length, the N-terminal half and the C-terminal half; Fig. 7C) were overexpressed in 293T cells, where no endogenous VEGFR-2 or VEGFR-3 was detected. Phosphorylation of VEGFR-3 was determined by a phosphor-specific antibody (pY1063/68, phosphorylation sites within the kinase activation loop essential for VEGFR-3 kinase activity [46, 47]. As shown in Fig. 7D, expression of AIP1-N strongly, while AIP1-F weakly, enhanced both total VEGFR-3 and phosphorylation of VEGFR-3. Again, VEGFR-3 mRNA was not affected (data not shown). The effects of AIP1 on VEGFR-3 expression and activity correlated with the association of AIP1 with VEGFR-3.

It has been shown that VEGFR-3 endocytosis and turnover is high in sprouting EC in the retina, and the endocytosis of VEGFR-3 is mediated by Dab2, the transmembrane protein Ephrin B2 and the cell polarity regulator Par-3[39, 40, 48]. Of note, AIP1 is also identified as a Dab2-interacting protein (Dab2IP). To test if AIP1 facilitates VEGFR-3 endocytosis and signaling, we determined the surface VEGFR-3 levels in AIP1 knockdown HLEC by FACS analyses and surface biotinylation assays as we recently described for VEGFR-2 [49]. VEGF-C induced VEGFR-3 endocytosis in HLEC, and the surface VEGFR-3 level was reduced by

50% at 5 min and 75% at 10 min after VEGF-C stimulation (Supplemental Fig. VI). However, AIP1 siRNA significantly attenuated VEGF-C-induced VEGFR-3 endocytosis at both 5 min and 10 min (Fig. 7E for 5 min; Supplemental Fig. VI for other time points). Similar results were obtained by surface biotinylation assay (Fig. 7F with quantifications in G).

VEGFR-3 protein level remains at a high level despite its fast endocytosis in the sprouting retinal EC[39, 40, 48]. The mechanism for the VEGFR-3 stability was unknown. We also examined if AIP1 regulates VEGFR3 half-life. To this end, VEGFR-3 stability in HLEC was examined in the presence of protein synthesis inhibitor cycloheximide. Cycloheximide reduced VEGFR-3 expression to 50% at 4 h, indicating VEGFR3 $T_{1/2}$ = 4h in Ctrl cells. However, in the AIP1 siRNA-treated HLEC VEGFR-3 level was reduced to 40% at 1h, indicating VEGFR3 $T_{1/2}$ is < 1h in AIP1-depleted cells (Fig. 7H). Further kinetic analyses indicated that VEGFR3 $T_{1/2}$ is = 30 min in AIP1 knockdown HLEC (Supplemental Fig. VII). As a control, VEGFR-2 stability was slightly increased by AIP1 knockdown, consistent with our previously observations[27, 37].

Discussion

In the present study, we have examined vascular development in the AIP1-deficient mice. We report that a global deletion or a vascular endothelial specific deletion of AIP1 reduces sprouting of retinal vessels which express both VEGFR-2 and VEGFR-3. In contrast, a neuronal cell-specific deletion of AIP1 has no adverse effects on retinal angiogenesis. The reduced VEGFR-3 signaling correlates with the retinal phenotype observed in the AIP1-KO mice. Consistently, AIP1-KO pups show defects in VEGFR-3-dependent developmental lymphangiogenesis in the skin and mesentery. Moreover, lymphangiogenesis in vivo (cornea lymphangiogenesis assay) and in vitro (human lymphatic EC migration) induced by a VEGFR-3-specific ligand mutant VEGF-C (C156Ser) is reduced by AIP1 deletion. Taken together, these results support an important role of AIP1 in VEGFR-3-dependent angiogenesis and lymphangiogenesis.

AIP1 differentially regulates VEGFR-2 and VEGFR-3

Our current finding were a surprise initially as we have previously observed that AIP1-deficient mice exhibit augmented pathological angiogenesis in several animal models. We demonstrate that AIP1, by blocking VEGFR-2 signaling, limits pathological angiogenesis. Mechanistically, AIP1 is recruited to the activated VEGFR-2/PI3K complex, leading to inactivation of the VEGFR-2 signaling[27]. Our current study supports that AIP1 differentially regulates VEGFR-3 and VEGFR-2 in sprouting vessels and lymphatic vessels. Specifically, AIP1 in VEGFR-2/3-expressing endothelial cells (e.g., human lymphatic EC) constitutively binds to VEGFR-3 in both resting and VEGF-C-treated EC; this binding enhances the VEGFR-3 endocytosis and protein stability in resting EC and the VEGFR-3 phosphorylation/activity in VEGF-C-treated cells. This conclusion is supported by the following observations: 1) VEGFR-3 total protein, but not its mRNA, is reduced in AIP1-KO tissues (the retina, mesentery and skin) and in AIP1-depleted mouse and human EC; 2) AIP1 knockdown accelerates VEGFR-3 degradation and shorten its half-life in HLEC; 3) AIP1 knockdown reduces the total VEGFR-3 level by 60–80%, but completely diminishes VEGF-C (C156Ser)-induced VEGFR-3 phosphorylation and downstream Akt activation, suggesting that AIP1 also plays a role in regulating VEGFR-3 activation; 4) finally, co-expression of AIP1 with VEGFR-3 in 293T cells lacking endogenous VEGFR-3 or VEGFR-2 indicates that AIP1 via its N-terminal half binds to VEGFR-3 and enhances VEGFR-3 autoactivation.

Mechanism by which AIP1 regulates VEGFR-3 expression/activity

It is known that VEGFR-3 expression is tightly regulated during vascular development as well as under pathological settings. VEGFR-3 is maintained in blood endothelial cell lymphatic precursors but becomes restricted to lymphatic endothelial cells with the exception of few blood capillaries in some organs [12]. VEGFR-3 protein can be regulated at multiple levels. The transcription factors Prox1, NF-κB, Ets and the transcription factor T-box 1 (Tbx1) transactivate the *Vegfr3* gene expression by directly binding to the *Vegfr3* gene promoter [50, 51]. Notch can also transactivate the *Vegfr3* gene [52], although some reports suggest negative regulations of VEGFR-3 expression by the Notch signaling [39, 40, 53]. We have recently shown that *miR-1236* binds to the 3′ untranslated region (UTR) of the *Vegfr3* mRNA and inhibits its translation, representing a post-transcriptional mechanism for VEGFR-3 expression [42]. The VEGFR-3 level is also regulated by protein stability. Dr. Adams' groups has reported that a strong increase in the VEGFR-3 but not the VEGFR-2 protein in Notch-defective (*Rbpj*-deletion and *Dll4*-deletion) angiogenic retinal vessels and lung vasculatures. However, the levels of VEGFR-3 mRNA were not substantially increased, suggesting a post-transcriptional regulation of VEGFR-3 by Notch. These results also suggest that VEGFR-2 and VEGFR-3 are differentially regulated despite their ability to form heterodimers [54]. Our present study has demonstrated that AIP1 modulates VEGFR-3 at several levels, including VEGFR-3 protein expression, and VEGFR-3 surface expression and stability. We do not observe increased Notch signaling in AIP1 deletion tissues or cells, therefore it is unlikely that AIP1 through Notch pathway regulates the VEGFR-3 expression. Instead, we observe that AIP1 deletion strongly induces expression of *miR-1236* in cultured EC, and likely AIP1 via *miR-1236* controls VEGFR-3 protein expression. We have previously reported that AIP1 deletion increases inflammation and cytokine expression [27, 29] and that cytokines induce *miR-1236* [52]. We propose that cytokines induced by the AIP1 deletion increases *miR-1236* expression to attenuate VEGFR-3 expression. Our study also reveals that AIP1 modulates VEGFR-3 surface expression and stability by direct AIP1-VEGFR-3 interactions. It has been shown that VEGFR-3 endocytosis is mediated by Dab2, the transmembrane protein Ephrin B2 and the cell polarity regulator Par-3[39, 40, 48]. A plausible model is that AIP1 (also named as DAB2IP) via Dab2 associates with the VEGFR-3 complex, facilitating its endocytosis and signaling. Meanwhile, AIP1 may also facilitate VEGFR-3 recycling or/and delay VEGFR-3 trafficking to lysosomes so that AIP1 maintains the surface and total levels of VEGFR-3. We are currently investigating this possibility.

Our current study also begs a question – what is biological significance of differential regulations of VEGFR-2 and VEGFR-3 by AIP1? While VEGF-A via VEGFR-2 primarily induces angiogenesis, VEGF-C via VEGFR-3 is more active in inducing lymphangiogenesis in vivo (cornea assay) and in vitro (the HLEC tube formation assay) [42–44]. For the downstream signaling, VEGF-C/VEGFR-3 induces a weaker phosphorylation of the PLC-γ axis, but shows a stronger activation of Akt compared to VEGF-A/VEGFR-2. It is now recognized that crosstalk (and mutual inhibition) between the PLC-γ/MAPK axis and the PI3K/Akt axis play an important role in the fate determination of artery, vein and lymphatic endothelial cells during development and pathological remodeling [55, 56]. It is possible that AIP1, by differentially regulating VEGFR-2/PLC-γ and VEGFR-3/Akt, controls the fine-tuning of vascular network formation. It is also recognized that pathological angiogenesis and lymphangiogenesis are differentially regulated during inflammation. Inflammation-induced angiogenesis occurs earlier than lymphangiogenesis, and lymphangiogenesis may play a critical role in inflammation resolution [57]. The major phenotype in AIP1 deficient mice is augmented inflammatory responses in several pathological models including ischemia and inflammation-induced angiogenesis. The VEGF-A/VEGFR-2 signaling not only controls angiogenesis, but also contributes to inflammatory responses by regulating

vascular permeability [58]. It is plausible that AIP1 limits inflammation by suppressing VEGF-A/VEFR-2-mediated vascular leakage at an early phase, and by enhancing VEGF-C/VEGFR-3-mediated lymphangiogenesis at a resolution phase. Therefore, AIP1 is a linker between inflammation and lymphangiogenesis, and may provide a novel target for the treatment of inflammation and lymphatic diseases.

Supplementary Material

Refer to Web version on PubMed Central for supplementary material.

Acknowledgments

Source of funding: This work was supported by NIH grants R01 HL065978, HL109420 and HL115148 to WM, and a National Nature Science Foundation of China (81371004) to ZX.

Abbreviations

AIP1	ASK1-interacting protein-1
AIP1-KO	AIP1-knockout mice
BrdU	5-bromo-2′-deoxyuridine
EC	endothelial cells
HLEC	human lymphatic EC
LYVE-1	lymphatic vessel endothelial hyaluronan receptor-1
siRNA	small interfering RNA
UTR	3′ untranslated region
VEGF-CS	vascular EC growth factor-C (C156Ser)
VEGFR2	vascular endothelial cell growth factor receptor-2
VEGFR3	vascular endothelial cell growth factor receptor-3)

References

1. Francois M, Caprini A, Hosking B, Orsenigo F, Wilhelm D, Browne C, Paavonen K, Karnezis T, Shayan R, Downes M, Davidson T, Tutt D, Cheah KS, Stacker SA, Muscat GE, Achen MG, Dejana E, Koopman P. Sox18 induces development of the lymphatic vasculature in mice. Nature. 2008; 456:643–647. [PubMed: 18931657]
2. Wigle JT, Oliver G. Prox1 function is required for the development of the murine lymphatic system. Cell. 1999; 98:769–778. [PubMed: 10499794]
3. Srinivasan RS, Geng X, Yang Y, Wang Y, Mukatira S, Studer M, Porto MP, Lagutin O, Oliver G. The nuclear hormone receptor coup-tfii is required for the initiation and early maintenance of prox1 expression in lymphatic endothelial cells. Genes Dev. 2010; 24:696–707. [PubMed: 20360386]
4. Karkkainen MJ, Haiko P, Sainio K, Partanen J, Taipale J, Petrova TV, Jeltsch M, Jackson DG, Talikka M, Rauvala H, Betsholtz C, Alitalo K. Vascular endothelial growth factor c is required for sprouting of the first lymphatic vessels from embryonic veins. Nat Immunol. 2004; 5:74–80. [PubMed: 14634646]
5. Breiteneder-Geleff S, Soleiman A, Horvat R, Amann G, Kowalski H, Kerjaschki D. podoplanin--a specific marker for lymphatic endothelium expressed in angiosarcoma. Verh Dtsch Ges Pathol. 1999; 83:270–275. [PubMed: 10714221]
6. Banerji S, Ni J, Wang SX, Clasper S, Su J, Tammi R, Jones M, Jackson DG. Lyve-1, a new homologue of the cd44 glycoprotein, is a lymph-specific receptor for hyaluronan. J Cell Biol. 1999; 144:789–801. [PubMed: 10037799]

7. Tammela T, Zarkada G, Wallgard E, Murtomaki A, Suchting S, Wirzenius M, Waltari M, Hellstrom M, Schomber T, Peltonen R, Freitas C, Duarte A, Isoniemi H, Laakkonen P, Christofori G, Yla-Herttuala S, Shibuya M, Pytowski B, Eichmann A, Betsholtz C, Alitalo K. Blocking vegfr-3 suppresses angiogenic sprouting and vascular network formation. Nature. 2008; 454:656–660. [PubMed: 18594512]
8. Halin C, Tobler NE, Vigl B, Brown LF, Detmar M. Vegf-a produced by chronically inflamed tissue induces lymphangiogenesis in draining lymph nodes. Blood. 2007; 110:3158–3167. [PubMed: 17625067]
9. Bjorndahl MA, Cao R, Burton JB, Brakenhielm E, Religa P, Galter D, Wu L, Cao Y. Vascular endothelial growth factor-a promotes peritumoral lymphangiogenesis and lymphatic metastasis. Cancer Res. 2005; 65:9261–9268. [PubMed: 16230387]
10. Nagy JA, Vasile E, Feng D, Sundberg C, Brown LF, Detmar MJ, Lawitts JA, Benjamin L, Tan X, Manseau EJ, Dvorak AM, Dvorak HF. Vascular permeability factor/vascular endothelial growth factor induces lymphangiogenesis as well as angiogenesis. J Exp Med. 2002; 196:1497–1506. [PubMed: 12461084]
11. Karpanen T, Alitalo K. Molecular biology and pathology of lymphangiogenesis. Annu Rev Pathol. 2008; 3:367–397. [PubMed: 18039141]
12. Tammela T, Alitalo K. Lymphangiogenesis: Molecular mechanisms and future promise. Cell. 2010; 140:460–476. [PubMed: 20178740]
13. Kaipainen A, Korhonen J, Mustonen T, van Hinsbergh VW, Fang GH, Dumont D, Breitman M, Alitalo K. Expression of the fms-like tyrosine kinase 4 gene becomes restricted to lymphatic endothelium during development. Proc Natl Acad Sci U S A. 1995; 92:3566–3570. [PubMed: 7724599]
14. Dumont DJ, Jussila L, Taipale J, Lymboussaki A, Mustonen T, Pajusola K, Breitman M, Alitalo K. Cardiovascular failure in mouse embryos deficient in vegf receptor-3. Science. 1998; 282:946–949. [PubMed: 9794766]
15. Tammela T, Zarkada G, Nurmi H, Jakobsson L, Heinolainen K, Tvorogov D, Zheng W, Franco CA, Murtomaki A, Aranda E, Miura N, Yla-Herttuala S, Fruttiger M, Makinen T, Eichmann A, Pollard JW, Gerhardt H, Alitalo K. Vegfr-3 controls tip to stalk conversion at vessel fusion sites by reinforcing notch signalling. Nat Cell Biol. 2011; 13:1202–1213. [PubMed: 21909098]
16. Karkkainen MJ, Ferrell RE, Lawrence EC, Kimak MA, Levinson KL, McTigue MA, Alitalo K, Finegold DN. Missense mutations interfere with vegfr-3 signalling in primary lymphoedema. Nat Genet. 2000; 25:153–159. [PubMed: 10835628]
17. Evans AL, Bell R, Brice G, Comeglio P, Lipede C, Jeffery S, Mortimer P, Sarfarazi M, Child AH. Identification of eight novel vegfr-3 mutations in families with primary congenital lymphoedema. J Med Genet. 2003; 40:697–703. [PubMed: 12960217]
18. Karkkainen MJ, Saaristo A, Jussila L, Karila KA, Lawrence EC, Pajusola K, Bueler H, Eichmann A, Kauppinen R, Kettunen MI, Yla-Herttuala S, Finegold DN, Ferrell RE, Alitalo K. A model for gene therapy of human hereditary lymphedema. Proc Natl Acad Sci U S A. 2001; 98:12677–12682. [PubMed: 11592985]
19. Shibuya M, Claesson-Welsh L. Signal transduction by vegf receptors in regulation of angiogenesis and lymphangiogenesis. Exp Cell Res. 2006; 312:549–560. [PubMed: 16336962]
20. Koch S, Tugues S, Li X, Gualandi L, Claesson-Welsh L. Signal transduction by vascular endothelial growth factor receptors. Biochem J. 2011; 437:169–183. [PubMed: 21711246]
21. Nakamura Y, Patrushev N, Inomata H, Mehta D, Urao N, Kim HW, Razvi M, Kini V, Mahadev K, Goldstein BJ, McKinney R, Fukai T, Ushio-Fukai M. Role of protein tyrosine phosphatase 1b in vascular endothelial growth factor signaling and cell-cell adhesions in endothelial cells. Circ Res. 2008; 102:1182–1191. [PubMed: 18451337]
22. Bruns AF, Herbert SP, Odell AF, Jopling HM, Hooper NM, Zachary IC, Walker JH, Ponnambalam S. Ligand-stimulated vegfr2 signaling is regulated by co-ordinated trafficking and proteolysis. Traffic. 2010; 11:161–174. [PubMed: 19883397]
23. Karpanen T, Heckman CA, Keskitalo S, Jeltsch M, Ollila H, Neufeld G, Tamagnone L, Alitalo K. Functional interaction of vegf-c and vegf-d with neuropilin receptors. Faseb J. 2006; 20:1462–1472. [PubMed: 16816121]

24. Simons M. An inside view: Vegf receptor trafficking and signaling. Physiology (Bethesda). 2012; 27:213–222. [PubMed: 22875452]
25. Chamorro-Jorganes A, Araldi E, Penalva LO, Sandhu D, Fernandez-Hernando C, Suarez Y. Microrna-16 and microrna-424 regulate cell-autonomous angiogenic functions in endothelial cells via targeting vascular endothelial growth factor receptor-2 and fibroblast growth factor receptor-1. Arterioscler Thromb Vasc Biol. 2011
26. Zhang R, He X, Liu W, Lu M, Hsieh JT, Min W. Aip1 mediates tnf-alpha-induced ask1 activation by facilitating dissociation of ask1 from its inhibitor 14-3-3. J Clin Invest. 2003; 111:1933–1943. [PubMed: 12813029]
27. Zhang H, He Y, Dai S, Xu Z, Luo Y, Wan T, Luo D, Jones D, Tang S, Chen H, Sessa WC, Min W. Aip1 functions as an endogenous inhibitor of vegfr2-mediated signaling and inflammatory angiogenesis in mice. J Clin Invest. 2008; 118:3904–3916. [PubMed: 19033661]
28. Xie D, Gore C, Liu J, Pong RC, Mason R, Hao G, Long M, Kabbani W, Yu L, Zhang H, Chen H, Sun X, Boothman DA, Min W, Hsieh JT. Role of dab2ip in modulating epithelial-to-mesenchymal transition and prostate cancer metastasis. Proc Natl Acad Sci U S A. 2010; 107:2485–2490. [PubMed: 20080667]
29. Yu L, Qin L, Zhang H, He Y, Chen H, Pober J, Tellides G, Min W. Aip1 prevents graft arteriosclerosis by inhibiting ifn-γ-dependent smooth muscle cell proliferation and intimal expansion. Cir Res. 2011; 109:418–427.
30. Huang Q, Qin L, Dai S, Zhang H, Pasula S, Zhou H, Chen H, Min W. Aip1 suppresses atherosclerosis by limiting hyperlipidemia-induced inflammation and vascular endothelial dysfunction. Arterioscler Thromb Vasc Biol. 2013; 33:795–804. [PubMed: 23413429]
31. Zhang H, Zhang R, Luo Y, D'Alessio A, Pober JS, Min W. Aip1/dab2ip, a novel member of the ras-gap family, transduces traf2-induced ask1-jnk activation. J Biol Chem. 2004; 279:44955–44965. [PubMed: 15310755]
32. Zhang H, Zhang H, Lin Y, Li J, Pober JS, Min W. Rip1-mediated aip1 phosphorylation at a 14-3-3-binding site is critical for tumor necrosis factor-induced ask1-jnk/p38 activation. J Biol Chem. 2007; 282:14788–14796. [PubMed: 17389591]
33. Wan T, Liu T, Zhang H, Tang S, Min W. Aip1 functions as arf6-gap to negatively regulate tlr4 signaling. J Biol Chem. 2010; 285:3750–3757. [PubMed: 19948740]
34. Gariano RF, Gardner TW. Retinal angiogenesis in development and disease. Nature. 2005; 438:960–966. [PubMed: 16355161]
35. Gerhardt H, Golding M, Fruttiger M, Ruhrberg C, Lundkvist A, Abramsson A, Jeltsch M, Mitchell C, Alitalo K, Shima D, Betsholtz C. Vegf guides angiogenic sprouting utilizing endothelial tip cell filopodia. J Cell Biol. 2003; 161:1163–1177. [PubMed: 12810700]
36. Sclafani AM, Skidmore JM, Ramaprakash H, Trumpp A, Gage PJ, Martin DM. Nestin-cre mediated deletion of pitx2 in the mouse. Genesis. 2006; 44:336–344. [PubMed: 16823861]
37. He Y, Zhang H, Yu L, Gunel M, Boggon TJ, Chen H, Min W. Stabilization of vegfr2 signaling by cerebral cavernous malformation 3 is critical for vascular development. Sci Signal. 2010; 3:ra26. [PubMed: 20371769]
38. Jakobsson L, Franco CA, Bentley K, Collins RT, Ponsioen B, Aspalter IM, Rosewell I, Busse M, Thurston G, Medvinsky A, Schulte-Merker S, Gerhardt H. Endothelial cells dynamically compete for the tip cell position during angiogenic sprouting. Nat Cell Biol. 2010; 12:943–953. [PubMed: 20871601]
39. Nakayama M, Berger P. Coordination of vegf receptor trafficking and signaling by coreceptors. Exp Cell Res. 2013; 319:1340–1347. [PubMed: 23499743]
40. Benedito R, Rocha SF, Woeste M, Zamykal M, Radtke F, Casanovas O, Duarte A, Pytowski B, Adams RH. Notch-dependent vegfr3 upregulation allows angiogenesis without vegf-vegfr2 signalling. Nature. 2012; 484:110–114. [PubMed: 22426001]
41. Norrmen C, Ivanov KI, Cheng J, Zangger N, Delorenzi M, Jaquet M, Miura N, Puolakkainen P, Horsley V, Hu J, Augustin HG, Yla-Herttuala S, Alitalo K, Petrova TV. Foxc2 controls formation and maturation of lymphatic collecting vessels through cooperation with nfatc1. J Cell Biol. 2009; 185:439–457. [PubMed: 19398761]

42. Jones D, Li Y, He Y, Xu Z, Chen H, Min W. Mirtron microrna-1236 inhibits vegfr-3 signaling during inflammatory lymphangiogenesis. Arterioscler Thromb Vasc Biol. 2012; 32:633–642. [PubMed: 22223733]
43. Jones D, Min W. An overview of lymphatic vessels and their emerging role in cardiovascular disease. J Cardiovasc Dis Res. 2011; 2:141–152. [PubMed: 22022141]
44. Jones D, Xu Z, Zhang H, He Y, Kluger MS, Chen H, Min W. Functional analyses of the nonreceptor kinase bone marrow kinase on the x chromosome in vascular endothelial growth factor-induced lymphangiogenesis. Arterioscler Thromb Vasc Biol. 2010; 30:2553–2561. [PubMed: 20864667]
45. Makinen T, Veikkola T, Mustjoki S, Karpanen T, Catimel B, Nice EC, Wise L, Mercer A, Kowalski H, Kerjaschki D, Stacker SA, Achen MG, Alitalo K. Isolated lymphatic endothelial cells transduce growth, survival and migratory signals via the vegf-c/d receptor vegfr-3. Embo J. 2001; 20:4762–4773. [PubMed: 11532940]
46. Fournier E, Blaikie P, Rosnet O, Margolis B, Birnbaum D, Borg JP. Role of tyrosine residues and protein interaction domains of shc adaptor in vegf receptor 3 signaling. Oncogene. 1999; 18:507–514. [PubMed: 9927207]
47. Salameh A, Galvagni F, Bardelli M, Bussolino F, Oliviero S. Direct recruitment of crk and grb2 to vegfr-3 induces proliferation, migration, and survival of endothelial cells through the activation of erk, akt, and jnk pathways. Blood. 2005; 106:3423–3431. [PubMed: 16076871]
48. Nakayama M, Nakayama A, van Lessen M, Yamamoto H, Hoffmann S, Drexler HC, Itoh N, Hirose T, Breier G, Vestweber D, Cooper JA, Ohno S, Kaibuchi K, Adams RH. Spatial regulation of vegf receptor endocytosis in angiogenesis. Nat Cell Biol. 2013; 15:249–260. [PubMed: 23354168]
49. Pasula S, Cai X, Dong Y, Messa M, McManus J, Chang B, Liu X, Zhu H, Mansat RS, Yoon SJ, Hahn S, Keeling J, Saunders D, Ko G, Knight J, Newton G, Luscinskas F, Sun X, Towner R, Lupu F, Xia L, Cremona O, De Camilli P, Min W, Chen H. Endothelial epsin deficiency decreases tumor growth by enhancing vegf signaling. J Clin Invest. 2012; 122:4424–4438. [PubMed: 23187125]
50. Flister MJ, Wilber A, Hall KL, Iwata C, Miyazono K, Nisato RE, Pepper MS, Zawieja DC, Ran S. Inflammation induces lymphangiogenesis through up-regulation of vegfr-3 mediated by nf-kappab and prox1. Blood. 2010; 115:418–429. [PubMed: 19901262]
51. Chen L, Fulcoli FG, Tang S, Baldini A. Tbx1 regulates proliferation and differentiation of multipotent heart progenitors. Circ Res. 2009; 105:842–851. [PubMed: 19745164]
52. Shawber CJ, Funahashi Y, Francisco E, Vorontchikhina M, Kitamura Y, Stowell SA, Borisenko V, Feirt N, Podgrabinska S, Shiraishi K, Chawengsaksophak K, Rossant J, Accili D, Skobe M, Kitajewski J. Notch alters vegf responsiveness in human and murine endothelial cells by direct regulation of vegfr-3 expression. J Clin Invest. 2007; 117:3369–3382. [PubMed: 17948123]
53. Niessen K, Zhang G, Ridgway JB, Chen H, Kolumam G, Siebel CW, Yan M. The notch1-dll4 signaling pathway regulates mouse postnatal lymphatic development. Blood. 2011; 118:1989–1997. [PubMed: 21700774]
54. Nilsson I, Bahram F, Li X, Gualandi L, Koch S, Jarvius M, Soderberg O, Anisimov A, Kholova I, Pytowski B, Baldwin M, Yla-Herttuala S, Alitalo K, Kreuger J, Claesson-Welsh L. Vegf receptor 2/-3 heterodimers detected in situ by proximity ligation on angiogenic sprouts. Embo J. 2010; 29:1377–1388. [PubMed: 20224550]
55. Deng Y, Atri D, Eichmann A, Simons M. Endothelial erk signaling controls lymphatic fate specification. J Clin Invest. 2013; 123:1202–1215. [PubMed: 23391722]
56. Deng Y, Larrivee B, Zhuang ZW, Atri D, Moraes F, Prahst C, Eichmann A, Simons M. Endothelial raf1/erk activation regulates arterial morphogenesis. Blood. 2013; 121:3988–3996. S3981–3989. [PubMed: 23529931]
57. Huggenberger R, Siddiqui SS, Brander D, Ullmann S, Zimmermann K, Antsiferova M, Werner S, Alitalo K, Detmar M. An important role of lymphatic vessel activation in limiting acute inflammation. Blood. 2011; 117:4667–4678. [PubMed: 21364190]
58. Weis SM, Cheresh DA. Pathophysiological consequences of vegf-induced vascular permeability. Nature. 2005; 437:497–504. [PubMed: 16177780]

Significance

- Using global and cell-specific AIP1 knockout mice, we show that endothelial AIP1, but not neuronal AIP1, is an important mediator in formation of new blood and lymphatic vessels.
- AIP1, a signaling adaptor molecule, modulates VEGFR-3 protein expression via miR-1236, and enhance VEGFR-3 activity and stability via direct binding to a surface receptor VEGFR-3 in endothelial cells.
- AIP1 may provide a novel target for the treatment of vascular and lymphatic diseases.

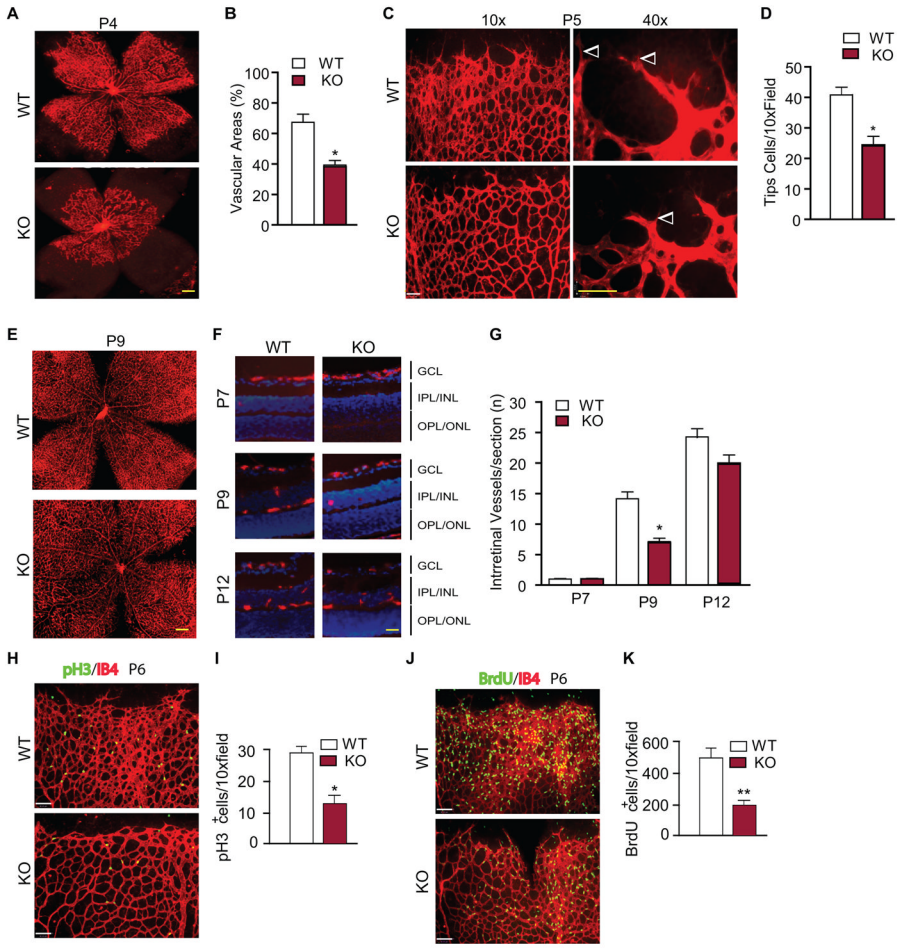

Figure 1. Effect of a global AIP1 deletion in retinal vascular development

Retinas from WT (AIP1$^{lox/lox}$) and the global AIP1-KO (AIP1$^{lox/lox}$:β-actin-Cre) at P3 to P17 were collected. **A–B**. The superficial retinal vasculatures were visualized by isolectin B4 staining. Images from P4 are shown (A). Scale bar: 500 μm. Vascularized areas were quantified as a percentage of the total retinal surface (B). n=10 retinas from 5 mice for each strain. **C–D**. Representative images of retina tips cells (indicated by arrowheads) from WT and AIP1-KO are shown (C). Scale bar: 50 μm. Tip cells were quantified (D). Data are mean ± SEM from 5 mice for each group. *, $p<0.05$ comparing AIP1-KO to WT. **E–G**. The superficial retinal vasculatures at P9 are shown (E). Scale bar: 500 μm. Intraretinal vessels from GCL into deeper IPL and OPL layers were examined by isolectin staining of eye cross sections. Images from P7, P9 and P12 are shown (F). Scale bar: 50 μm. Intraretinal vessel number/section was quantified (G). Data are mean ± SEM from 3 sections of each retina and 10 retinas from 5 mice for each group. *, $p<0.05$ comparing AIP1-KO to age-match WT. **H–I**. P6 retinas were subjected to whole mount staining with isolectin for EC (red) and phosphor-histone-3 (pH3) for proliferative cells (green). Representative images are shown (H). Scale bar: 50 μm. pH3-positive cells are quantified (I). Data are mean ± SEM from 3 pairs of WT and AIP1-KO. *, $p<0.05$ comparing AIP1-KO to age-match WT. **J–K**. P6 WT and AIP1-KO mice were injected with BrdU for 2 h and retinas were subjected to whole-mount staining with isolectin for EC (red) and anti-BrdU for proliferative cells (green). Representative images are shown (J). Scale bar: 50 μm. BrdU-positive cells are quantified (K). Data are mean ± SEM from 3 pairs of WT and AIP1-KO. *, $p<0.05$ comparing AIP1-KO to age-match WT.

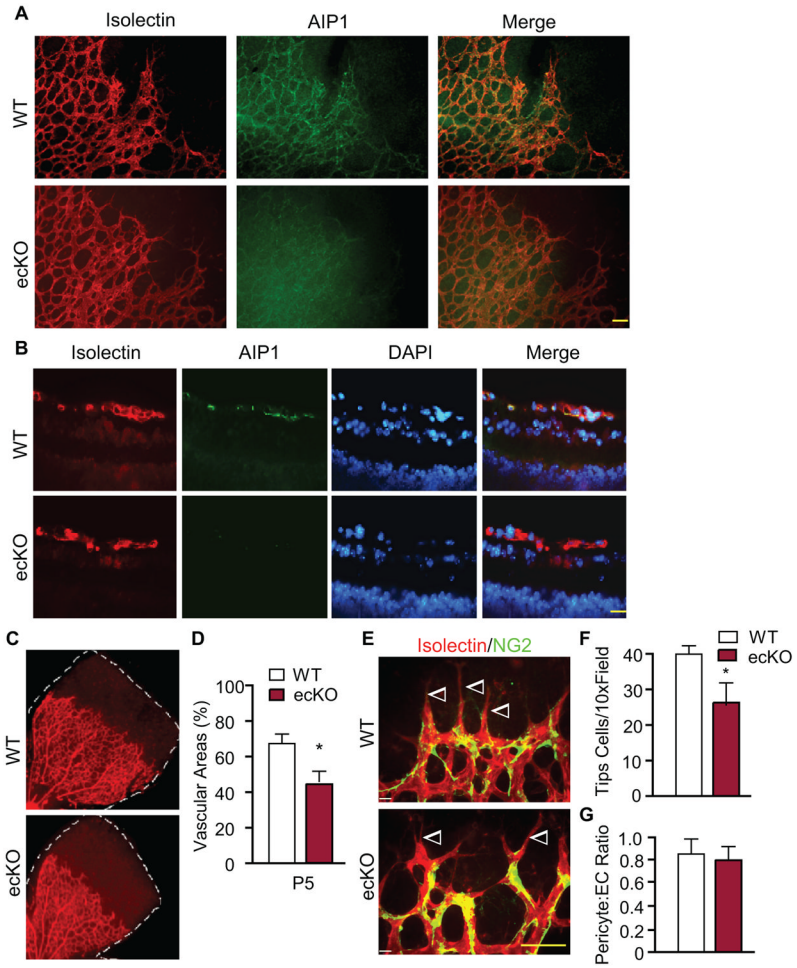

Figure 2. Effect of an endothelial-specific AIP1 deletion in retinal vascular development

P5 retinas from WT (AIP1$^{lox/lox}$) and the AIP1-ecKO (AIP1$^{lox/lox}$:Tie2-Cre) were collected. **A–B**. AIP1 expression and EC-specific deletion in AIP1-ecKO retinas were detected by immunostaining of whole mounting (A) and cross sections (B) by anti-AIP1 together with isolectin B4 staining. Scale bar: 50 μm. **C–D**. The superficial retinal vasculatures were visualized by isolectin staining (C). Vascularized areas were quantified as a percentage of the total retinal surface (D). n=10 retinas from 5 mice for each strain. *, $p<0.05$ comparing AIP1-KO to WT. **E–F**. P5 retinas were subjected to whole-mount staining with isolectin for EC (red) and NG2 for pericytes (green). Representative images of retina tips cells (indicated by arrowheads) are shown (E). Scale bar: 50 μm. Tip cells were quantified (F). Data are mean ± SEM from 5 mice for each group. *, $p<0.05$ comparing AIP1-KO to WT. **G.** Numbers of pericytes (NG2-positive) and EC (isolectin-positive) were quantified and the ratios of pericyte:EC are presented.

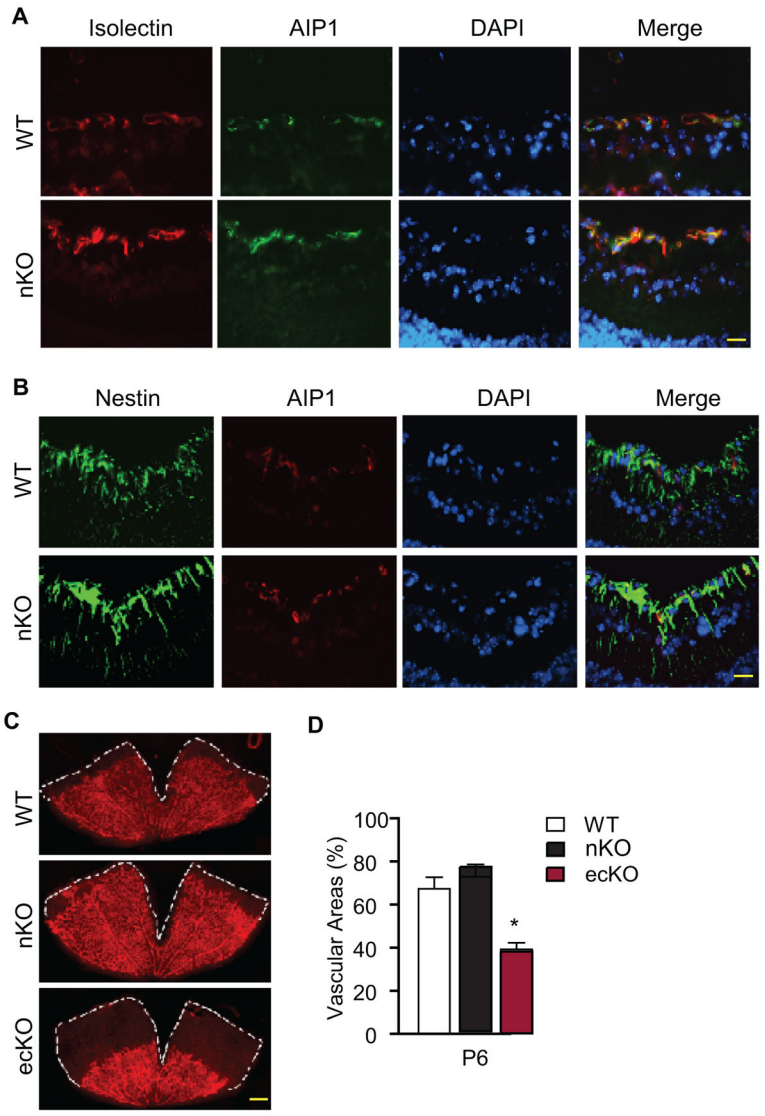

Figure 3. Effect of a neuronal-specific AIP1 deletion in retinal vascular development

P6 retinas from WT (AIP1$^{lox/lox}$), the AIP1-nKO (AIP1$^{lox/lox}$:Nestin-Cre) and the AIP1-ecKO (AIP1$^{lox/lox}$:Tie2-Cre) were collected. **A–B**. AIP1 expression was detected by immunostaining of cross sections by anti-AIP1 together with isolectin staining (for EC) or nestin staining (for neuronal cells).). Scale bar: 50 μm. **C–D**. The superficial retinal vasculatures were visualized by isolectin staining (C). Scale bar: 500 μm. Vascularized areas were quantified as a percentage of the total retinal surface (D). n=10 retinas from 5 mice for each strain. *, $p<0.05$ comparing AIP1-ecKO to WT. No significance was detected comparing AIP1-nKO to WT group.

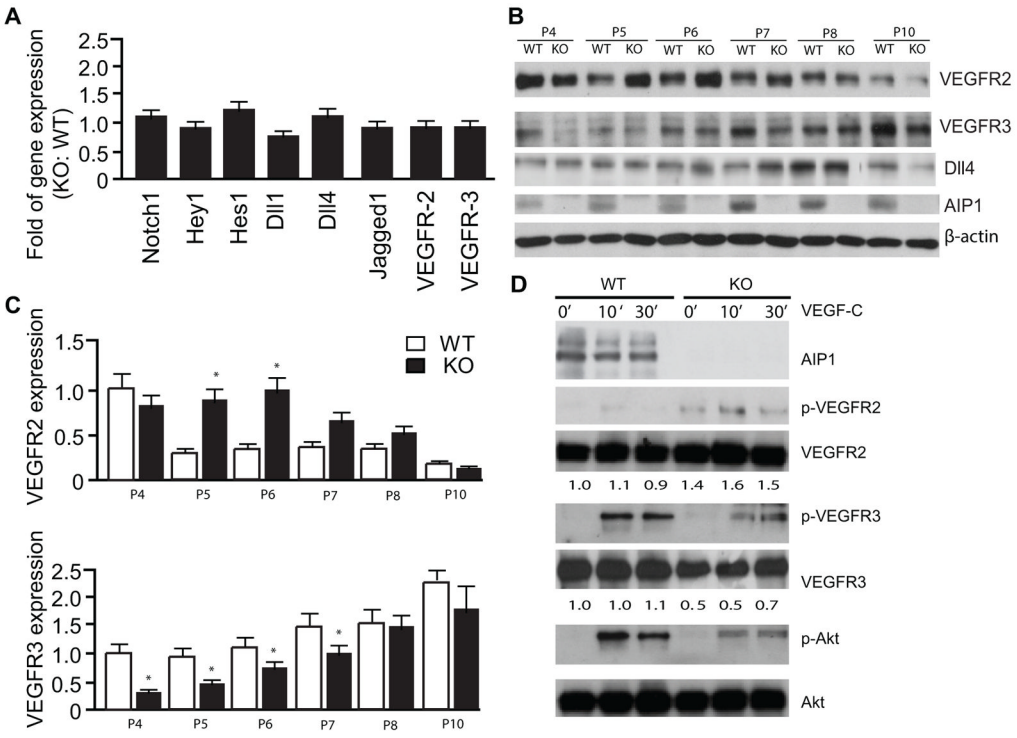

Figure 4. VEGFR-3, but not VEGFR-2 or Notch signaling, is specifically reduced in AIP1-KO retinas

A. Retinas from WT and AIP1-KO at P5 were collected. Gene expression of VEGFR-2, VEGFR-3 and Notch signaling molecules were determined by qRT-PCR. Data represent fold changes by taking WT as 1.0. Data are mean ± SEM from 6 retinas for each group. **B–D**. Protein expression of VEGFR-2, VEGFR-3 and Notch signaling molecules. Retinas from WT and AIP1-KO at P4-P10 were harvested. Protein expressions were determined by immunoblotting with respective antibodies. Representative blots from four independent experiments are shown in B. Relative levels of VEGFR-2 and VEGFR-3 expression are represent by taking WT P4 as 1.0. Data are mean ± SEM from 6 retinas for each group. *, $p<0.05$ comparing AIP1-KO to WT. **D**. Effects of AIP1 deletion on VEGF-C signaling. Retinal EC were isolated from P7 retinas and were serum-starved overnight. Cells were treated with VEGF-C (100 ng/ml) for indicated times. Phosphorylations of VEGFR-2, VEGFR-3 and Akt were determined by Western blot with phosphor-specific antibodies. Total protein levels of VEGFR-2, VEGFR-3, Akt and AIP1 were determined by Western blot with respective antibodies. Relative levels of VEGFR-3 and VEGFR-2 are indicated below the blot with untreated WT group as 1.0. Similar results were obtained from additional two experiments.

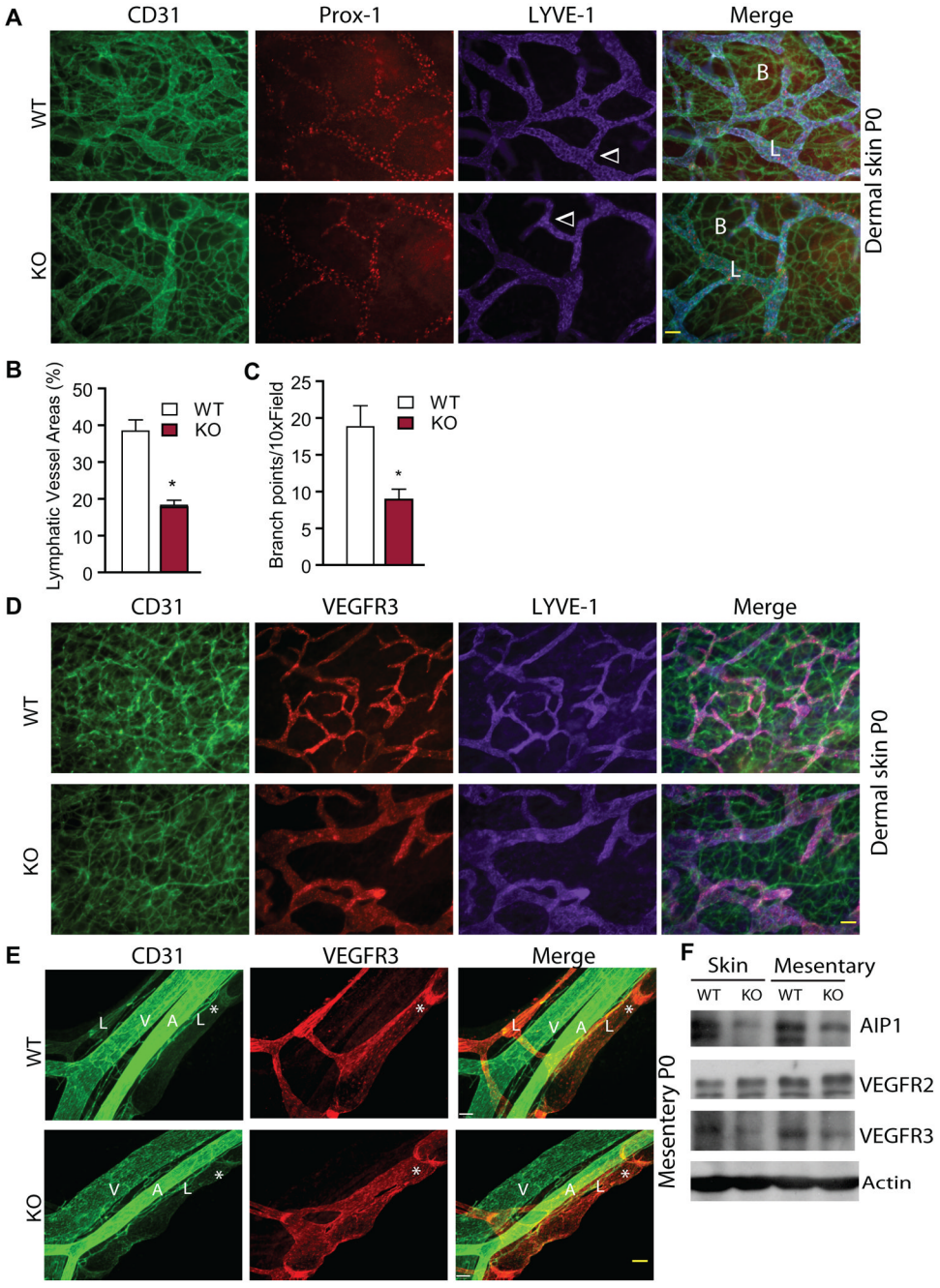

Figure 5. AIP1 deletion delays lymphangiogenesis in neonatal skin and mesentery

Dermal skin and mesentery from WT and AIP1-KO at P0 were collected. **A.** Blood and lymphatic vessels in dermal skin were visualized by whole-mount immunostaining with anti-CD31 (green), anti-Prox-1 (red) and anti-LYVE-1 (purple). Merged images are shown on the right. Blood and lymphatic vessels as well as lymphatic vessel branches are indicated. Scale bar: 50 μm. **B–C**. % of lymphatic vessel areas (B) and lymphatic vessel branches (C) were quantified. n=3 sections from 3 mice for each strain. *, $p<0.05$ comparing AIP1-KO to WT. **D**. Blood and lymphatic vessels in dermal skin were visualized by whole mount immunostaining with anti-CD31 (green), anti-VEGFR-3 (red) and anti-LYVE-1 (purple). Merged images are shown on the right. Scale bar: 50 μm. **E**. Representative whole-mount

immunostaining of mesenteric vessels with anti-CD31 (green), anti-Prox-1 (red) and anti-LYVE-1 (purple). Merged images are shown on the right. A: artery; V: vein; L: lymphatics. The lymphatic valves are indicated by *. Scale bar: 50 μm. **F.** Protein expression of VEGFR-3. Skin and mesentary tissues from WT and AIP1-KO at P0 were harvested. Protein expressions were determined by immunoblotting with respective antibodies. Representative blots from four independent experiments are shown.

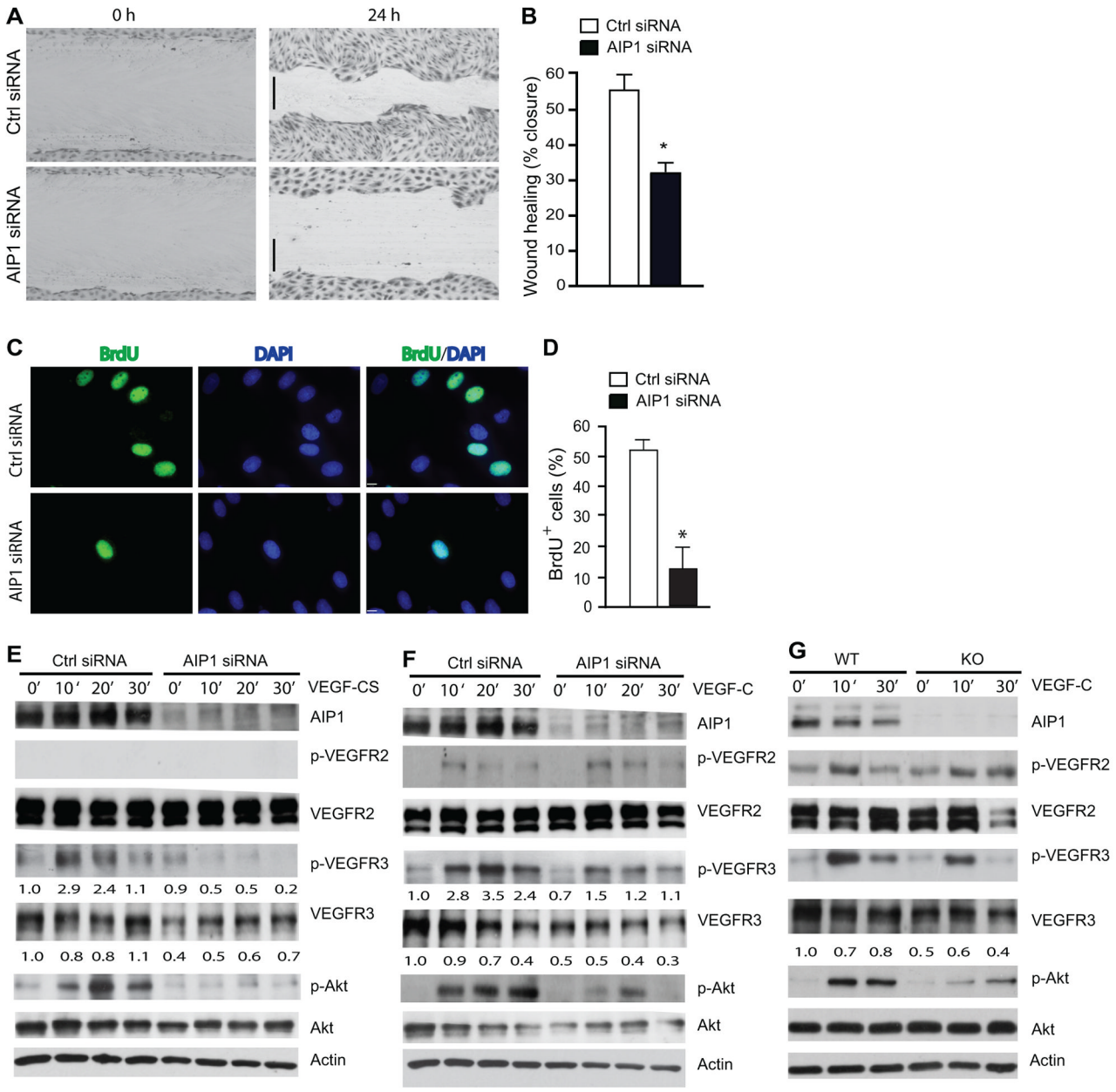

Figure 6. AIP1 mediates VEGF-C-induced lymphangiogenic signaling

A–B. HLEC monolayer migration assay. 48 h after transfection with Ctrl or AIP1 siRNA, confluent monolayers of HLEC were subjected to "wound" injury assay in the presence of 3% serum + VEGF-CS (250 ng/ml) for 24 h. Representative images are shown in A. Scale bar, 100 μm. Cell migration distances (mm) were measured and % wound closure was quantified in B. Data are mean±SEM from duplicates (10 different areas in each well) of three independent experiments. *, $P<0.05$. **C–D**. BrdU incorporation assay. 48 h after transfection with Ctrl or AIP1 siRNA, HLEC were subjected to BrdU labeling for 4 h followed by immunostaining with anti-BrdU. Representative images are shown in C and BrdU+ cells were quantified in D. Data are mean±SEM from duplicates (5 different areas in slide) of three independent experiments. *, P<0.05. **E–F**. Effects of AIP1 knockdown in VEGF-CS- and VEGF-C signaling. HLEC were transfected with a human AIP1 siRNA or

control siRNA (20 nM) for 24 h, subsequently serum-starved overnight. Cells were treated with VEGF-CS (250 ng/ml) or VEGF-C (100 ng/ml) for indicated times. Knockdown of AIP1 was determined by Western blot with anti-AIP1. Phosphorylations of VEGFR-2, VEGFR-3 and Akt were determined by Western blot with phosphor-specific antibodies. Total levels of VEGFR-2, VEGFR-3 and Akt were determined by Western blot with respective antibodies. β-actin was used as a loading control, and relative levels of p-VEGFR-3 and total VEGFR-3 are indicated below the blot with untreated Ctrl group as 1.0. Similar results were obtained from additional two experiments. **G.** Effects of AIP1 deletion on VEGF-C signaling. Mouse dermal lymphatic EC were isolated. Cells were cultured and treated with VEGF-C as in F for indicated times. Phosphorylations of VEGFR-2, VEGFR-3 and Akt were determined by Western blot with phosphor-specific antibodies. Total protein levels of VEGFR-2, VEGFR-3, Akt and AIP1 were determined by Western blot with respective antibodies. Similar results were obtained from additional two experiments.

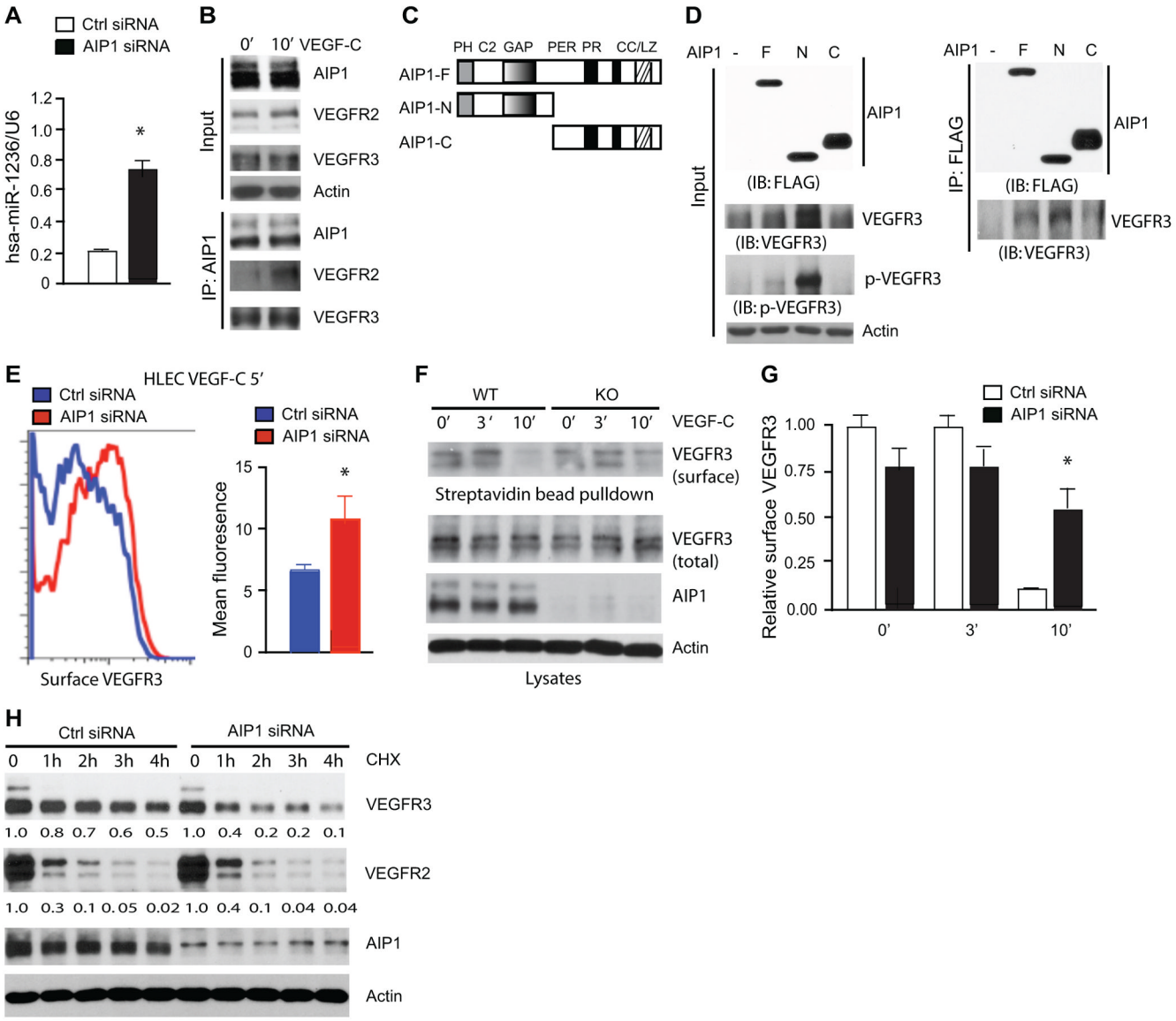

Figure 7. AIP1 mediates VEGFR-3 protein expression and activation

A. Effects of AIP1 knockdown on miR-1236 expression in HLEC. HLEC were transfected with Ctrl or AIP1 siRNA (20 nM) for 48 h. TaqMan primers were used to probe miR-1236 expression, which was normalized to RNU6B expression using the comparative Ct method. Data are mean ± SEM from duplicates in three independent experiments. *, $p<0.05$. **B.** Association of endogenous AIP1 with VEGFR-2 and VEGFR-3. HLEC were serum-starved and treated with VEGF-C (100 ng/ml for 10 min). Associations of AIP1 with VEGFR-2 and VEGFR-3 were determined by a co-immunoprecipitation assay with anti-AIP1 followed by Western blot with anti-VEGFR-2 or anti-VEGFR-3. Proteins in the input were determined by Western blot with respectively antibodies. Experiments were repeated twice. **C.** Schematic diagram for AIP1 structural domains and expression constructs. (AIP1-F: the full length; AIP1-N: the N-terminal half contains a PH, a C2 and a Ras-GAP domain; AIP1-C: the C-terminal half containing a period-like domain, a proline-rich motif and a coiled coil/ leucine-zipper domain). PH: plekstrin homolog domain; C2: PKC-conserved region 2; GAP: Ras GTPase-activating protein domain; PER: period-like domain; PR: proline-rich motif;

CC/LZ: coiled coil/leucine-zipper domain. **D.** AIP1 via its N-terminal half binds to and stabilizes VEGFR-3. VEGFR-3 expression plasmid was co-transfected with FLAG-tagged AIP1-F, AIP1-N or AIP1-C into 293T cells. Phospho- and total VEGFR-3 were determined by Western blot with specific antibodies. Associations of AIP1 proteins with VEGFR-3 were performed by co-immunoprecipitation with anti-FLAG followed by Western blot with anti-VEGFR-3. (−): vector control. **E**. Effects of AIP1 knockdown on VEGFR-3 surface expression. HLEC were transfected with Ctrl or AIP1 siRNA (20 nM) for 48 h. HLEC were treated with VEGF-C (100 ng/ml) for indicated times. Surface VEGFR-3 was detected by FACS with anti-VEGFR-3. Representative FACS for VEGF-C 5 min group is shown. **F–G**. Cell-surface VEGFR-3 was labeled by cell-surface biotinylation, and analyzed by streptavidin bead pull-down followed by Western blotting with antibodies indicated. Relative VEGFR-3 surface (ratio of surface VEGFR-3/total VEGFR-3) was quantified in G. Data are mean ± SEM from three independent experiments. *, $p<0.05$. **H**. Effects of AIP1 knockdown on VEGFR-3 half-life. HLEC were transfected with Ctrl or AIP1 siRNA (20 nM), 48 h after transfection, HLEC were treated with cycloheximide (10 μg/ml) for indicated times. Total levels of VEGFR-3, VEGFR-2, AIP1 and β-actin were determined by Western blot with respective antibodies. Relative levels of total VEGFR-3 and VEGFR-2 are indicated below the blot with untreated Ctrl group as 1.0. Similar results were obtained from additional two experiments.